A Study of Design of Hollow Fiber Membrane Modules for using in Artificial Lung by the PZT Actuator

Gi Beum Kim[1,2,3,4], Seong Jong Kim[5], Chul Un Hong[2,3,4], Yong Chul Lee[6], Min Ho Kim[1,7]

[1]*Research Institute of Clinical Medicine, Chonbuk National University Medical School.*
[2]*Research Center of Industrial Technology, Chonbuk National University*
[3]*Research Center of Silver Engineering Technology, Chonbuk National University*
[4]*Division of Bionics and Bioinformatics, College of Engineering, Chonbuk National University*
[5]*Department of Bio & Applied Chemistry, Iksan National Collage*
[6]*Department of Internal Medicine, Airway Remodeling Laboratory, Chonbuk National University Medical Schools, and National Research Laboratory Program of the Korea Science and Engineering Foundation*
[7]*Department of Thoracic and Cardiovascular Surgery, Medical Schools, Chonbuk National University*
(Received January 6, 2006. Accepted July 31, 2006)

Abstract

The purpose of this work was to assess and quantify the beneficial effects of gas exchange, while testingto the various frequencies of the sinusoidal wave that was excited by the PZT actuator, for patients suffering from acute respiratory distress syndrome (ARDS) or chronic respiratory problems. Also, this paper considered a simulator to design a hollow type artificial lung, and a mathematical model was used to predict a behavior of blood. This simulation was carried out according to the Montecarno's simulation method, anda fourth order Runge-Kutta method was used to solve the equation. The experimental design and procedure are then applied to the construction of a new device to assess the effectiveness of the membrane vibrations. As a result, the vibration method is very effective in the increase of gas transport. The gas exchange efficiency for the vibrating intravascular lung assist device can be increased by emphasizing the following design features: consistent and reproducible fiber geometry, and most importantly, an active means of enhancing convective mixing of water around the hollow fiber membranes. The experimental results showed the effective performance of the vibrating intravascular lung assist device. Also, we concluded that important design parameters were blood flow rates, fiber outer diameter and oxygen pressure drop. Based on the present results, it was believed that the optimal level of blood flow rates was 200cm^3/min.

Key words : artificial lung, PZT actuator, mass transfer, ARDS, hemolysis

I. INTRODUCTION

Acute respiratory distress syndrome (ARDS) is a form of acute respiratory failure caused by extensive lung injury following a variety of catastrophic events such as shock, severe infection, or burns. ARDS can occur in individuals with or without previous lung disease.

Especially, respiratory failure usually occurs following a catastrophic event in individuals with no previous lung disease, not responding to ordinary methods of respiratory support. Regardless of the event causing the lung injury, the patients exhibit common signs and symptoms, x-ray findings, and tissue changes. Because many of its features resembled those of respiratory distress syndrome in newborns (RDS), the adult disease is referred to as ARDS.

The disease affects approximately 150,000 people per year in the United States [1]. Its treatment requires respiratory support using the conventional therapies of mechanical ventilation, or extracorporeal membrane oxygenation (ECMO) in patients with severe ARDS. The positive airway pressures and volume excursions associated with mechanical ventilation can result in further damage to lung tissue, including barotrauma, volutrauma and parenchyma damage due to the toxic levels of oxygen required for effective mechanical ventilation [2]. The alternative use of ECMO is complicated and expensive, requiring extensive blood/biomaterial contact in extracorporeal circuits, systemic anticoagulation, and labor-intensive patient monitoring. Due to these complications,

This work was supported by Korea Research Foundation Grant (KRF-2006-521-D00619).
Corresponding Author : Gi-Beum Kim
Division of Bionics and Bioinformatics, College of Engineering, Chonbuk National University, 664-14 1ga Dukjin-dong, Dukjin-Gu, Chonju, Chonbuk, 561-756, Republic of Korea
Tel : +82-63-250-2246 / Fax : +82-63-250-2236
E-mail : kgb70@chonbuk.ac.kr

the mortality rate of ARDS patients remains high, exceeding 50% [3, 4, 5, 6, 7, 8].

Intravascular oxygenation represents an attractive, alternative support modality for patients with ARDS. The concept of intravascular oxygenation as an alternative ARDS therapy originated with Mortensen [9], who developed an intravenous oxygenator (IVOX) consisting of a bundle of crimped hollow fiber positioned in the vena cava. In phase I clinical trials, the IVOX provided an average of 28% of the basal gas exchange requirements for patients with severe ARDS [10]. The clinical study, however, concluded that more gas exchange was needed for intravascular oxygenation to be clinically effective in ARDS treatment. Herein, an intravenous membrane oxygenator was developed, with a design goal of 50% of the base oxygen and carbon dioxide exchange requirements for end-stage ARDS patients. Similarly to IVOX, the intravenous membrane oxygenator consists of a bundle of manifold hollow fiber, and is intended for intravenous placement within the superior and inferior vena cava. Due to the target level of gas exchange required in the intravenous membrane oxygenator, the intravenous membrane oxygenator consequently incorporates a vibrating actuator concentric with the fiber bundle, thus enhancing the gas exchange. Our current efforts focused on device improvements intended to provide the target levels of gas exchange, taking into account the constraints imposed by intravenous placement on the fiber bundle size, and hence the fiber area, for gas exchange.

Although critical care techniques have been improved, the high mortality of severe acute respiratory failure (ARDS) has not significantly changed [11, 12].

In an intravenous membrane oxygenator, the greater part of the oxygen transfer resistance is located in the blood-side laminar film [13], and various methods have been tried to make the laminar film thinner and improve the oxygen transfer rate [14, 15, 16, 17]. In the present study, the water flow characteristics in the implantable artificial lung were evaluated by in vitro experiments methods [18].

Also, increasing into life support mechanism for people hasbeen conducted, owing to the recent development of science and technology. An artificial oxygenator is the product of one of these studies. The old artificial oxygenator was evolvedfrom a type of bubble oxygenator to a type of membrane, in which a membrane oxygenator was developed from a type of multilayer to a type of hollow fiber membrane. A hollow fiber membrane oxygenator used in open-heart surgery is commercialized in some foreign countries, and has been developed in Korea. The development of a type of membrane oxygenator requires a huge scale of analyzing equipment, and various knowledges. In addition, clinical experimentation for this product is difficult [19].

In this work, an analytical solution were developed for the hydrodynamics of the flow through a bundle of sinusoidally vibrated hollow fibers to provide some insight into how wall vibrations might enhance the performance of an intravascular lung assist device. Scaling analysis was then used to infer the dimensionless groups that correlate the performance of a vibrated hollow tube membrane oxygenator. The experimental design and procedure are then given for a device for assessing the effectiveness of membrane vibrations.

II. THEORY

For the Reynolds numbers, the dimensionless rate of mass transfer, K, is given by

$$K = N_{Sh} N_{Sc}^{-1/3} = f_1(N_{\mathrm{Re}}) = \alpha N_{\mathrm{Re}}^{-\beta} = \frac{p d N_{Sc}^{2/3}}{4(1-p)(P_b - P)} \qquad (1)$$

The Reynolds number, N_{Re} (=dv/υ), characterizes the flow regime and is the ratio of the inertial to viscous forces. The Schmidt number, N_{Sc} (=υ/D), analogous to the Prandtl number in heat transfer, characterizes the fluid properties and is to ratio of momentum to diffusive transports. The Peclet number, N_{Pe} (=dv/D), which is the product of N_{Re}, characterizes the relative importance of the convective and diffusive processes and is the ratio of bulk to diffusive mass transports. The Sherwood number, N_{Sh} (=Kd/D), also known as the mass transfer Nusselt number, likewise characterizes the relative importance of the convective and diffusive transports; it is the ratio of the total to diffusive transports. In the above definitions, d is the characteristic length, v the velocity, D the diffusivity, υ the kinematic viscosity and K the mass transfer rate [20, 21, 22, 23].

Equation 1 can express as following.

$$\frac{dP}{dx} = a \frac{P_b - P}{[1+\lambda(P)]^{2/3}} \qquad (2)$$

$$a = \frac{4}{p} \times \left(\frac{1-p}{d}\right)^{(1+\beta)} \times \left(\frac{A_f \eta}{Q\rho}\right)^{\beta} \times \frac{\alpha}{(v/D)^{2/3}} \qquad (3)$$

$$\lambda(P) = \frac{1.34}{k} C_{Hb} \frac{n}{P_{50}} \left(\frac{P}{P_{50}}\right)^{n-1} \frac{1}{[1+(P/P_{50})]^{n-2}} \qquad (4)$$

$$\eta_P = \frac{\exp[-5.64 + \frac{0.18\times10^4}{T+273}]}{100} \quad (5)$$

$$\eta = \eta_P \exp(2.31\mathrm{Hct}) \quad (6)$$

$$\rho = 1.09\mathrm{Hct} + 1.035(1-\mathrm{Hct}) \quad (7)$$

$$D_P = 1.62\times10^{-5}\times1.025^{(T-25)} \quad (8)$$

$$D_C = 0.76\times10^{-5}\times1.025^{(T-25)} \quad (9)$$

which P_{50} is partial pressure of oxygen at which the hemoglobin is 50% saturated with oxygen, n is Hiss parameter, η is high strain-rate absolute viscosity, η_p is high strain-rate absolute viscosity of plasma, T is temperature, ρ is blood density, D_P is diffusivity of a gas in plasma, and D_C is diffusivity of a gas in red blood cell.

If is case of person 26blood, from equation (2) to (9) are decided by following empirical equation.

$$n = 2.7 \quad (10)$$

$$P_{50}^{'} = 26.6\times10^{(0.48)(7.4-\mathrm{pH})} \quad (11)$$

$$P_{50} = P_{50}^{'}\times10^{(0.024)(37-T)} \quad (12)$$

But, if is case of bovine blood, from equation (2) to (9) are decided by following empirical equation.

$$n = 2.85 \quad (13)$$

$$P_{50}^{'} = 29.0\times10^{(0.41)(7.4-\mathrm{pH})} \quad (14)$$

$$P_{50} = P_{50}^{'}\times10^{(0.024)(37-T)} \quad (15)$$

Characteristic length is given by

$$d = \frac{\varepsilon}{1-\varepsilon} d_o \quad (16)$$

in which ϵ is the device porosity and d_o the outside diameter of hollow fiber membrane.

The O_2 content and O_2 transfer rate were calculated by the following standard formulas:

$$\mathrm{O_2\ content(vol\%)} = \frac{\mathrm{Hb}\times1.34\times\%\mathrm{O_2\ saturation}}{100}\times P_{\mathrm{O_2}}\times0.003 \quad (17)$$

$$\mathrm{O_2\ transfer\ rate(ml/min)} = (C_{aO_2} - C_{vO_2})\times\mathrm{liquid\ flow\ rate} \quad (18)$$

in which Hb is the hemoglobin (g/ml) and P_{O_2} the partial pressure of oxygen (mmHg), with 1.34 and 0.003 the ml of oxygen that could be carried by 1mg of hemoglobin, and that dissolved for each 1mmHg, respectively, and C_{aO_2} and C_{vO_2} the arterial and venous oxygen contents (vol %), respectively; the blood flow rate represents the pump flow rate (L/min).

Blood hemolysis was expressed as Normalized Index of Hemolysis (NIH) according to the equation [25, 26, 27, 28]:

$$\mathrm{NIH(g/100L)} = \frac{\Delta\mathrm{fHb}\times V\times(1-\frac{\mathrm{Ht}}{100})\times100}{\Delta t\times Q} \quad (19)$$

in which △fHb is the increase in free plasma hemoglobin concentration (g/L) during the testing time (min), Ht is the hematocrit (%), V the blood volume of each circuit (L) and Q the flow rate expressed in L/min.

III. MATERIALS AND METHODS

A. Blood Condition

The blood was obtained from cattle having normal body temperature, no physical signs of disease, including diarrhea or rhinorrhea, and an acceptable range of hematological

Table 1. Inlet parameters recommended by AAMI/ASTM Standard: Admitted range, minimum and maximum values measured during the test

	AAMI recommended range	Measured		
		Average	min	max
T (℃)	37±1	37.0	36.8	37.2
B.E. (mmol/L)	0±5	1.1	−1.8	2.7
SvO2 (%)	65±5	65.5	64.0	68.0
Hb (g/ml)	12±1	12.0	11.6	12.5

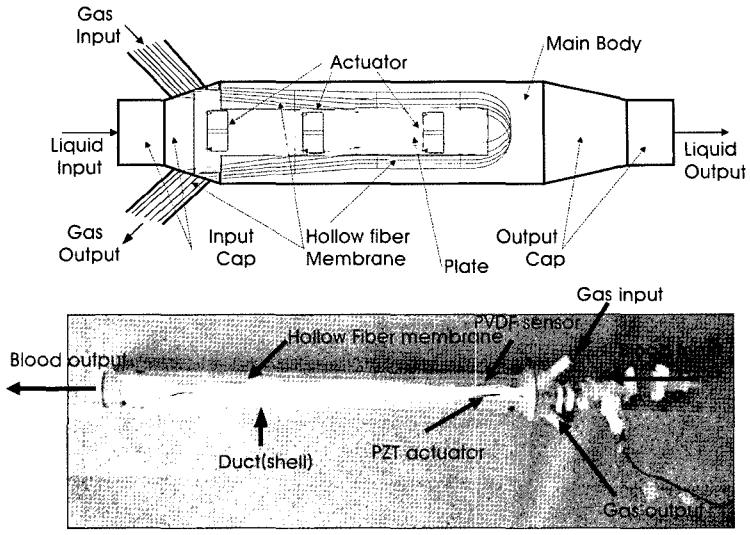

Fig. 1. Vibrating intravenous lung assist device.

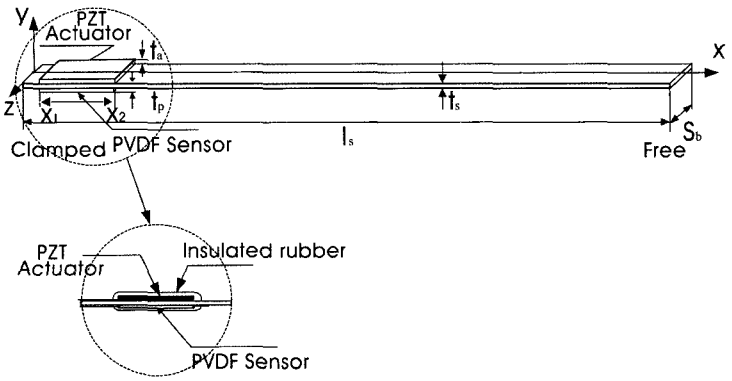

Fig. 2. Configuration of a cantilevered composite beam with piezo-film sensor and piezo-ceramic actuator.

profiles. The blood is collected by vascular puncture using a 14G needle, and put into 500mL blood bags containing a citrate phosphate dextrose adenine (CPDA-1) anticoagulant solution.

Before testing, the blood was examined to check for damaged samples. As shown in Table 1 the initial mean free hemoglobin concentration was 5.33±2.75mg/ml, and the mean hematocrit 28.1±3.0%. The blood was stored in a refrigerator during transportation and kept refrigerated upon arrival at our laboratory. All of the units of blood were used within 6 hours of acquisition.

B. Membrane Oxygenator

In this study, the experimental data were measured to evaluate the performance of the Vibrating Intravacular Lung Assist Device (VIVLAD). The test section was a cylinder duct with an axial length and inner diameter of 60 and 30 mm, respectively. Fig. 1 shows a photograph of the VIVLAD. The VIVLAD used for this experiment was prepared with the number of hollow fiber in the acryl cylinder as shown in Fig. 2. The VIVLAD was made of microporous polypropylene with an inner diameter and membrane thickness of 380 μm and 50 μm (Oxyphane, Enka, Germany), respectively. The experimental set-up of the flexible beam used in the artificial lung device is shown in Fig. 2. The PVDF sensor was a 28 μm thickness LDT1-028K (AMP Co.). The piezoceramic sensor used for the test module was a multi-layer bender PZT actuator (40×10×0.45 mm) which was a PL-128.255 Lead Zirconate Titanate (PZT) from Digtal ECHO company. The PZT actuator and PVDF sensor were bonded to the flexible beam with araldite adhesive, with the electrical leads soldered to the electrode of piezo-elements, and then covered with elastic rubber for waterproofing. The description of the VIVLAD is shown in Table 2.

C. Test Circuit

Fig.3 shows a photograph and drawing of the experimental closed loop for gas performance tests. The experimental

Table 2. Dimensions of hollow fiber modules

Parameter	Type 1	Type 2	Type 3	Type 4	Type 5
Membrane	Hollow fiber	Hollow fiber	Hollow fiber	Hollow fiber	Hollow fiber
Material	PP	PP	PP	PP	PP
Cylinder Duct Inner Diameter (mm)	30	30	30	30	30
Number of Hollow fiber	100	200	300	450	675

closed loop blood circuit consisted of 3/8 inch inner diameter biocompatibility tubing, a deoxygenator (Baxter Healthcare Corporation, Irvine, CA, USA), an electromagnetic blood flow meter and a roller pump (Cobe Cardiovascular, Inc., Arvada, Co. USA), which were used as the membrane oxygenator for this work. A gas blender (Sechrist Industries, Inc., Anaheim, CA) was connected to the deoxygenator with tube. The blood temperature wad maintained at 37℃ with a heat exchanger.

D. Oxygen Transfer Measurement

The measurements were performed in line with the AAMI/ISO international standard recommendations [28]. The experimental closed loop was primed with less than 6 liters of fresh filtered cattle blood after addition of 75 ml ADC and 1 ml heparin as anticoagulants. The hemoglobin content was calibrated to the required value (12.0±1.0 g/ml) by dilution of the blood with normal saline. Adequate recirculation was performed before the test, to adjust the blood's inlet conditions to those of the AAMI/ISO standards (Table.1). The test lasted six hours. Both the mean blood flow rate (Qb=6.0L/min or smaller) and the systolic period of the vibration waveform (50% of the entire cycle) were kept constant. Gas flow rates of up to 6 L/min through the 120-cm-long hollow fibers have been achieved by exciting a piezo-vibrator with a sinusoidal wave magnitude of DC 50 V. Fig. 3 shows the experimental setup of the testing equipment for measurement of the blood oxygen transfer. The experiment was carried out using a DSP 1104 board (TMS320C40, dSPACE GmbH, Germany) and an amplifier (SQV 3/150, Pizomechanik Dr. L. Piekehman GmbH, Germany). The signal from an A/D converter, with a sampling ratio of 1ms, was sent to the DSP system and the calculated input voltage to a PZT actuator, for exciting the test module through the D/A converter and amplifier.

The signals from the sensor, according to the applied input voltage, were digitalized and filtered in order to obtain the dynamic characteristics of the composite beam in the artificial lung device. In the filtering operation, the DC offset was rejected and the noise eliminated by band-pass filters (BPF) with the cutoff frequencies of 0.5 and 50Hz, respectively. Finally, thesignals are integrated to take into account the applied input voltage. The processed signals of the sensor output were obtained in real time on a personal computer.

Experiments were performed with various frequencies applied to the PZT actuator of the test module, which was bonded to the flexible beam in the artificial lung device. The dynamic response of the sensor system was obtained by applying the dynamic input voltage with varying frequencies of sinusoidal wave, from 0 to 50 Hz, and magnitudes of the excited input from 0 to 100V. The measuring system was discredited at sampling intervals of 0.001s. Every hour, excitation of the test module frequency (f) was varied, spanning 0 to 10Hz (step 1Hz), in four runs of 60 minutes each. In each run, three veno-arterial blood samples were

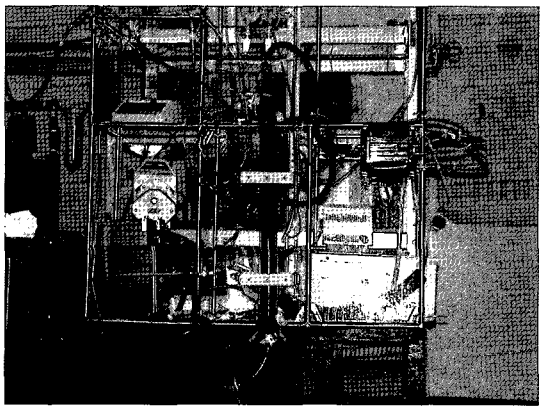

Fig. 3. The experimental circuit for the evaluation of oxygen transfer with bovine blood.

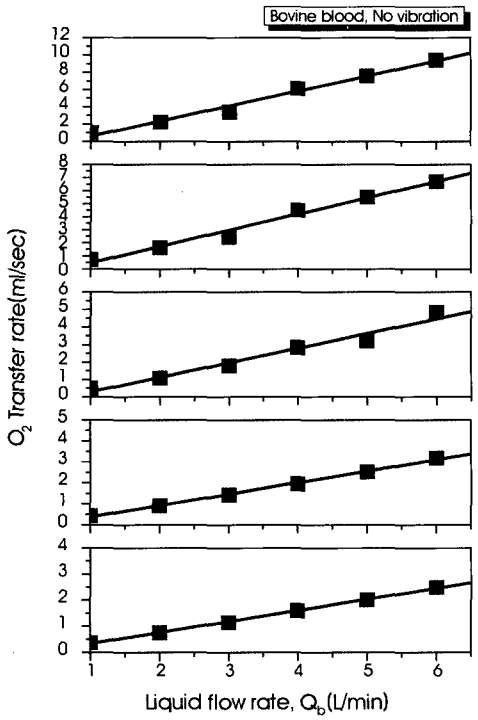

Fig. 4. Oxygen transfer rate for the VIVLAD, with various module types and liquid flow rates, using bovine blood, with no vibration.

withdrawn and immediately analyzed. The test VIVLAD was ventilated with 100% O_2, at a flow rate one time that of the blood flow. Samples were taken from the inlet and outlet sampling ports, and the blood gases analyzed with an i-Stat Portable Blood Gas/Electrolyte Analyzer (i-Stat Co., East Windser, NJ, USA). The O_2 and CO_2 transfer rates were calculated from the gas analysis data and blood flow rates. The data collection consisted of recordings of the venous and arterial oxygen saturation values (SvO_2, SaO_2), oxygen partial pressure (pvO_2, paO_2), venous and arterial pH, and total hemoglobin (Hb) in the exhausted gas.

E. Modeling Method

The computer used in the modeling of a mass transfer model was Pentium IV 1.8GHz, and the program used in this modeling was the Visual C++ 6.0. The whole algorithm consisted of the following:

Step 1. Various process parameters, such as pH, T, m, n, Hct, p, k, N, Q, L, and d are inputted in a dialog box of the input window.

Step 2. Various physical properties are calculated.

Step 3. Solve a differential equation using the Runge-Kutta fourth-order method. In the case of modeling that uses human blood, modeling will be conducted using Eqs. (2) ~ (9), and (10) ~ (12). For bovine blood, the modeling will be performed by using Eqs. (2) ~ (9), and (13) ~ (15).

Step 4. Each solution will be presented in the main window.

Step 5. Saving the graph as a meta file, makes it easy to open and print out.

Ⅳ. RESULTS AND DISCUSSION

Fig. 4 shows the relationships between the oxygen transfer and various blood flow rates without an excited vibration. When the blood flow rate increases, the oxygen transfers rate increases, and the module type 5 showed a higher oxygen transfer rate than any other modules. In addition, the pressure drop in the intravenous artificial lungs assist must keep lower than 15mmHg. Therefore, when the blood flow rate was 6 L/min, there were 675 hollow fibers in the cylinders available for insertion, with an inner diameter of 3 cm.

The mass transfer rate itself is reported as a Sherwood number, N_{Sh} (=Kd/D). The variations in the distilled water velocity and module length are reported as a Reynolds number, N_{Re}. Note that the characteristic diameter d is not always defined in exactly the same way, as explained in the "Remarks" column of the table. Note that the kinematics viscosity, υ, and the diffusion coefficient, D, have nor been varied in our experiments. Our correlations represent a

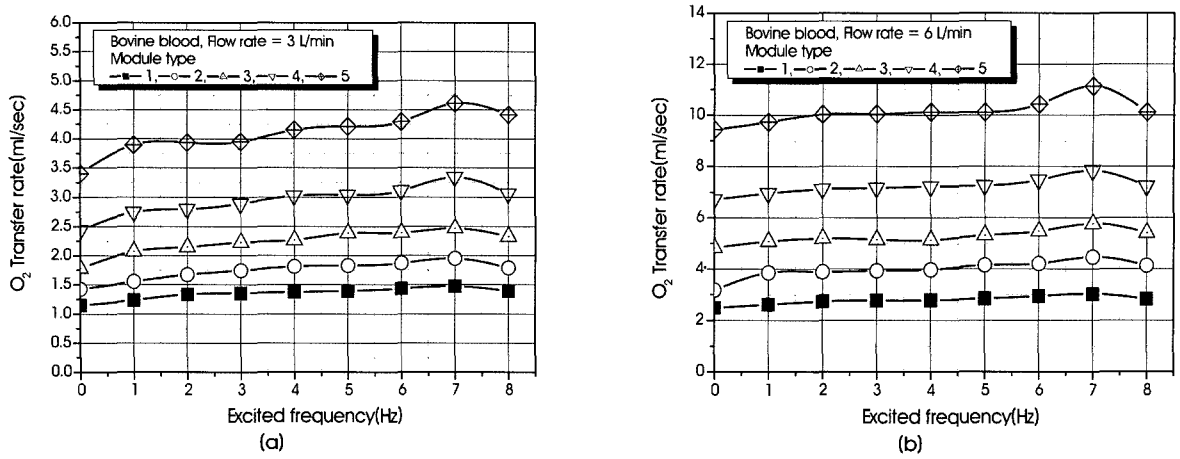

Fig. 5. Experimental circuit for the evaluation of the oxygen transfer in bovine blood. Oxygen transfer rate for the various VIVLAD module types, with the liquid flow rate varied, using bovine blood at various excited frequencies. (Blood flow rate (a) 3L/min, (b) 6L/min).

hypothesis based on the literature results.

For parallel flow outside of hollow fibers, our results do not agree with the previous correlations for this unbaffled laminar flow, so that answer was obviously due to some type of secondary flow, which was volunteered as the rationale by the heat transfer experts consulted. However, these same experts could not suggest specific references to support this idea. The oxygen transfer rate of the VIVLAD increased with increases in the number of tied hollow fibers, due to the more effective blood contact with the membrane. The water flow in the VIVLAD was not uniform and depended on the hollow fiber packing density. Stagnation of the water flow also occurred in the bundle of hollow fibers at the water inlet.

Fig. 5 shows the relationships between the excited frequency and oxygen transfer rate on the blood flow rate with the various module types. When the excited frequency increases, the oxygen transfer rate increases. However, although the oxygen transfer rate of propagation expressed a maximum when frequency was 7Hz, with frequencies greater than 7Hz the oxygen transfer rate of propagation again show decreasing tendencies. The reason for this could be judged and confirm from Fig. 5, where the frequency of 7Hz expressed a maximum oxygen velocity of propagation as the maximum flicker occurred in the blood of the fluid system. The maximum oxygen transfer rate seemed to be caused by the occurrence of the maximum amplitude and transfer of vibration to the hollow fiber when excited by a frequency of 7Hz for each blood flow rate, because this frequency became the 2nd mode resonance frequency of the flexible beam in blood flow. Therefore, the bandwidth of the excited frequency in Fig. 5 was shown to be up to 10Hz as the frequency bandwidth for the maximum oxygen transfer rate. The excited frequency for the maximum oxygen transfer rate at DC50V was 7Hz. With an excited frequency greater than 8Hz, the oxygen transfer rate was relatively low compared to that of 7Hz, but was similar to that of 6Hz. It was also shown that the oxygen transfer rate increased in each excited frequency bandwidth compared to the rate without vibration. There was

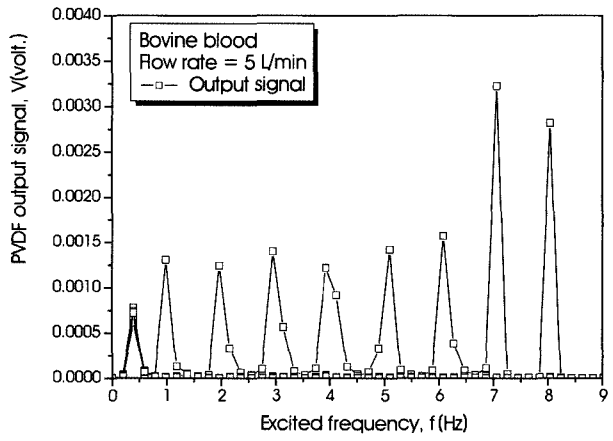

Fig. 6. Amplitude of PVDF sensor output for the system with various excited frequencies using bovine blood.

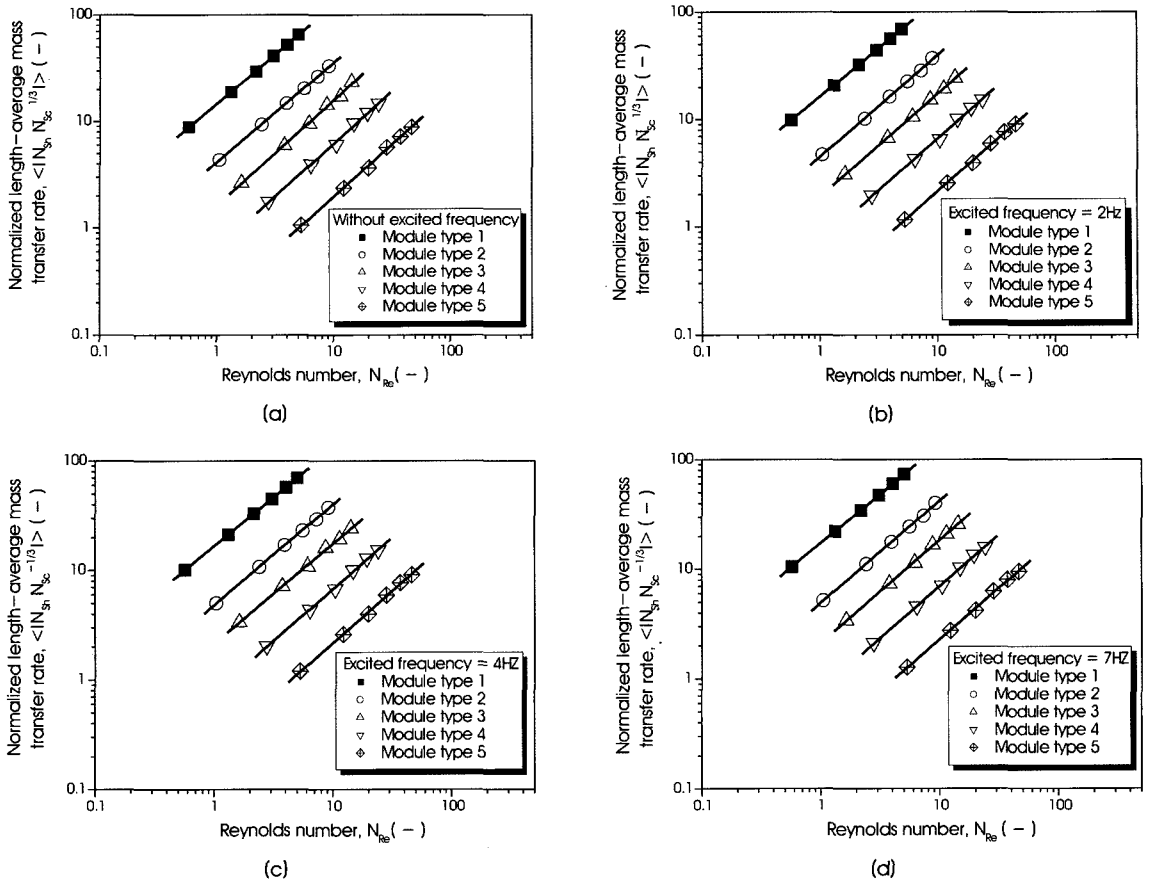

Fig. 7. Oxygenation performance of the various VIVLAD module types, using bovine blood, at various excited frequencies. ((a) without excited, (b) 2Hz, (c) 4Hz anc (d) 7Hz).

little difference between the oxygen transfer rates regardless of the vibration when the blood flow rate was relatively low; for instance, at 1L/min. However, the increments in the blood flow rate affect the oxygen transfer rate significantly. There was a large resonance affect on the oxygen transfer rate at a high blood flow rate, 6L/min, as there was a large resonance between the excited frequency of the flexible beam and the blood flow rate with an excited frequency of 7Hz. The resonance effect indicates doubled effects due to the coupling of the excited frequency of the test module and the blood flow. However, the array of the effective hollow fiber membrane was initially quite important, because the effect of oxygen transfer changed according to the contact states between the hollow fiber membrane and the blood.

Fig. 6 shows the output voltage of the PVDF sensor at the maximum oxygen transfer rate in module type 4. As shown in this Fig., the maximum amplitude of the PVDF sensor output was at a frequency band of 7Hz for various blood flow rates. The maximum oxygen transfer effect occurred at the frequency band of 7Hz. This resonance effect represented the maximum oxygen transfer rate by reducing the boundary layer, occurring on the surface of the hollow fiber membrane.

Fig. 7 shows the dependence of the mass transfer rate K of the blood flow in the VIVLAD at various excited vibrations. The mass transfer rate increased with the linear velocity of the blood flow. A lower number of tired hollow fibers produce a higher mass transfer rate at a constant blood-side flow velocity. These results indicate that the packing of hollow fiber strongly affects the mass transfer rate. This figureis a log-log plot of K vs. NRe for the experiment using the VIVLAD by varying the numbers of tied hollow fibers.

Least-squares fits yield the following equations:

$$
\begin{aligned}
K &= \alpha N_{\mathrm{Re}}^{\beta} \\
\alpha &= y_0 + A e^{-f/t} \\
y_0 &= 0.52 + 58.47 e^{-P^*/0.03} \\
A &= -0.07 - 5.47 e^{-P^*/0.04} \\
t &= 2.48 + 0.0001 e^{-P^*/0.22}
\end{aligned}
\tag{5}
$$

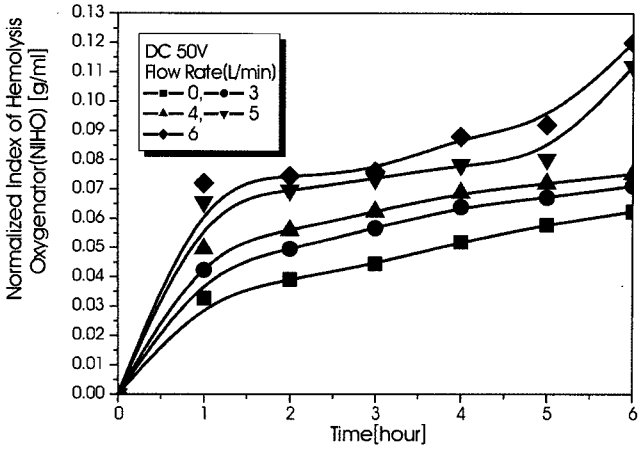

Fig. 8. Graph reveals variation in the plasma free hemoglobin with various blood flow rates over the passage of time at an excited frequency of 7Hz.

$$\beta = A' + B' x \tag{6}$$

$$A' = 0.98 - 0.31 e^{-p^*/0.02}$$

$$B' = 0.004 - 0.012 p^*$$

These values for the slope and vertical position are used in the equation $K = \alpha N_{\mathrm{Re}}^{\beta}$ to predict the O2transfer rates in water for the VIVLAD with various numbers of tied hollow fibers.

Fig. 8 shows the relationship between the changes in the plasma free hemoglobin and time at different flow rates in module type 5, indicating the maximum oxygen transfer rate. Fig. 8 shows the changes in the plasma free hemoglobin with each PZT actuator activated with the sinusoidal wave amplitude of DC10V. The change in the plasma free hemoglobin was 0.112g/ml after 6 hours with the sinusoidal wave amplitude of DC10V and an excited frequency band of 7Hz at the blood flow rate of 5L/min in module type 5. From the results of the hemolysis, it was determined that damage to blood does not occur because the hemolysis is low,which was measured during the 6 hours of excitation in frequency region of 7Hz in the experiment. Enhancing the performance of the contactors using the membrane vibrations also offers an additional advantage of minimizing fouling. Employing membrane vibrations may be more amenable to enhancing the performance of an implantable blood oxygenator because it is easier to implement and is less traumatic than when employing direct pulsations of the fluid flow.

Fig. 9 presents the results of a modeling, which was varied by blood flows, outside diameter of the hollow fiber membrane, and pressure difference of oxygen. The most effective parameter for the length of the artificial oxygenator or the area of the membrane among the parameters was the change of blood flow. By considering specific phenomenon in the lung, in particular control of the differences in the pressures of

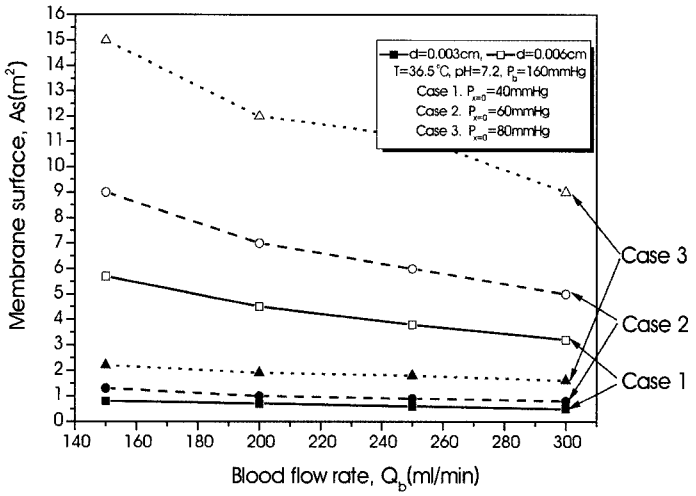

Fig. 9. Blood flow rate vs. membrane surface.

oxygen inside or outside of the lung, it is much easier to control the outside diameter of a hollow fiber membrane than that of the blood flows. Using this, it was possible to obtain results from the modeling that act as a function of the lung, and changes the blood flows as shown from the results presented from Fig. 9. That is, the rates of the changes in the length of device, or the area of membrane were small. Therefore, it was reasonable that the configuration of the blood flows was 200cm^3/min. This can be estimated using previously applied theoretical equations. From the results of the modeling, the rates of changes in the length of device or the area of membrane were small at flows over 200cm^3/min in the process condition, which initiated the same difference in pressure (55mmHg). Therefore, it was reasonable that the configuration of the blood flows was 200cm^2/min. In addition, these results indicate that the smaller outside diameter of the hollow fiber membrane showed a shorter length for the device. Because the Mockros model was produced using a dimension analyzing model, which used the relationship of data that was acquired by the existing commercial models, such as the SMO1, Turbo, and Univox Mockros, it was possible to present some severe errors between the estimated and the measured values in the case of using the other company's model.

V. CONCLUSIONS

This study represents the limit of blood hemolysis, which is produced by the vibration techniques used to improve the oxygen transfer efficiency in the new type artificial lung assist device. As a result, the effect of the various excitation frequencies in gas transfer rates and hemolysis could measures using the maximum gas transfer rate. The maximum oxygen transfer rate was reached through the occurrence of maximum amplitude, and the transfer of a vibration to the hollow fiber membranes. This is because this frequency was the 2nd mode resonance frequency of the flexible beam, which was also bundled with 675 hollow fiber membranes in the blood flow. Therefore, it was determined that the limit of the hemolysis frequency was the frequency band of 7Hz, because the maximum amplitude was obtained from the PVDF sensor at this frequency. The results reported above strongly indicate that mass transfer almost always controls the performance of microporous hollow-fibers in the blood phase. This study indicated that the most important design parameters in the design of a type of hollow fiber membrane artificial oxygenator were the blood flows, outside diameter of the hollow fiber membrane, and the pressure difference of oxygen. All situations that could be performed in some tests were modeled using the Montecarlos modeling method, and integrated by using the Runge-Kutta fourth-order method. Considering certain phenomenon in the lung, the most important parameter in the design of an artificial oxygenatorthe blood flow, in which the blood flow of 200cm^3/min showed an optimal process condition.

REFERENCE

[1] W. J. Fedespiel, M. S. Hout, T. J. Hewitt, L. W. Lund, S. A. Heinrich, P. Litwak, F. R. Walters, G. D. Reeder, H. S. Borovetz, and B. G. Hattler, "Development of a low flowresistance intravenous oxygenator," *ASAIO J.*, vol. 43, pp. M725-M730, 1997.

[2] S. E. Weinberger, Principles of Pulmonary Medicine. Philadelphia: Saunders, 1992.

[3] L. Gattinoni, A. Pesenti, and G. P. Rossi, "Treatment of acute respiratory failure with low-frequency positive-pressure ventilation and extracorporeal removal of CO_2," *Lancet*, vol. 2, pp. 292-294, 1980.

[4] A. Pesenti, L. Gattinoni, T. Kobolow, and G. Damia, "Extracorporeal circulation in adult respiratory failure, " *ASAIO Trans.*, vol. 34, pp. 43-47, 1988.

[5] M. T.Snider, D. B. Campbell, W. A. Kofke, K. M. High, G. B. Russell, M. F. Keamy, and D. R. Williams, "Venovenous perfusion of adult and children with severe acute respiratory distress syndrome," *ASAIO Trans.*, vol. 34, pp. 1014-1020, 1988.

[6] T. G. Campell, "Changing criteria for the artificial lung: Historic controls on the technology of ECMO," *ASAIO J.*, vol. 40, pp. 109-120, 1994.

[7] S. Ichiba, and R. H. Bartlett, "Current status of extracorporeal membrane oxygenation for severe respiratory failure", *Artif. Organs*, vol. 20, pp. 120-123, 1996.

[8] T. J. Hewitt, B. G. Hattler and W. J. Federspiel, "A mathematical model of gas exchange in an intravenous membrane oxygenator," *Ann. Biomed. Eng.*, vol. 26, pp. 166-178, 1998.

[9] J. D. Mortensen, "Intravascular oxygenator: A new alternative method for augmenting blood gas transfer in patient with acute respiratory failure," *Artif. Organs*, vol. 16, pp. 75-82, 1992.

[10] S. A. Conrad, "Major findings from the clinical trials of the intravascular oxygenator," *Arti. Organs*, vol. 18, pp. 846-863, 1994.

[11] M. A. Woodhead, "Management of pneumonia," *Respir. Med.*, vol. 86, pp. 459-469, 1992.

[12] T. T. Nguyen, J. B. Zwischenberger, W. Tao, D. I. Traber, D. N. Herndon, C. C. Duncan, B. Push, and A. Bidani, "Significant enhancement of carbon dioxide removal by a new prototype IVOX," *ASAIO J.*, vol. 39, pp. M719-724, 1993.

[13] S. N. Vaslef, L. F. Mockros, R. W. Anderson, and R. J. Leonard, "Use of a mathematical model to predict oxygen transfer rates in hollow fiber membrane oxygenators," *ASAIO J.*, vol. 40, pp. 990-996, 1994.

[14] H. M. Weissman, and L. F. Mockros, "Gas transfer to blood flowing in coiled circular tubes," *J. Eng. Mech. Div. ASCM*, vol. 94, pp. 857-872, 1968.

[15] K. Tanishita, P. D. Richardson, and P. M. Galletti, "Tightly wound coils of microporous tubing: progress with secondary flow blood oxygenator design," *Trans. ASME,* vol. 21, pp. 216-222, 1975.

[16] G. B. Kim, T. K. Kwon, G. R. Jheong, and S. C. Lee, "Gas Transfer and Hemolysis Characteristic of a New Type Intravenous Lung Assist Devices," *J. Biomed. Eng. Res.*, vol. 24, no. 2, pp. 121-126, 2003.

[17] G. B. Kim, T. K. Kwon, and C. U. Hung, "Design of an Intravenous Oxygenator," *J. Artif. Organs*, vol. 9, no. 1, pp. 34-41, 2006.

[18] V. L. Streeter, E. B. Wylie, and K. Bedford, *Fluid Mechanics* (9th ed.), New York: McGrew-Hill Inc., 1998.

[19] G. B. Kim, S. J. Kim, C. U. Hong, T. K. Kwon, and N. G. Kim, "Enhancement of Oxygen Transfer in Hollow Fiber Membrane by the Vibration Method," *Korean J. Chem. Eng.*, vol. 22, no. 4, pp. 521-527, 2005.

[20] M. Mulder, *Basic Principles of Membrane Technology*, New York: Kluwer Academic Publishers, pp. 418-422, 1996.

[21] M. T. Snider, "Clinical trails of an intravenous oxygenator in patients with adult respiratory distress syndrome," *Anesthesoilogy*, vol. 77, pp. 855-863, 1972.

[22] W. L. Beek, K. M. K. Muttzell, and J. W. van Heuven, *Transport Phenomena* (2th ed.), Singapore: John Wiley & Sons Inc., pp. 262-267, 1999.

[23] R. B. Bird, W. E. Stewart, and E. N. Lightfoot, *Transport Phenomena* (2th ed.), New York: John Wiley & Sons Inc., pp. 675-677, 2002.

[25] P. J. Morin, C. Gosselin, R. Picard, M. Vincent, R. Giundoin, and C. I. H. Nicholl, "Implantable artificial lung," *J. Thorac. Cardivasc. Surg.*,vol. 74, pp. 130-136, 1977.

[26] K. Naito, K. Mizuguchi, and Y. Nosé, "The Need for Standardizing the Index of Hemolysis," *Artif. Organs*, vol. 18, pp. 7-10, 1994.

[27] Y. Nosé, "Recommended practice for assessment of hemolysis in continuous flow blood pump west conshohoken," *P.A. American Society of Testing and Materials*, pp. 40-41, 1998.

[28] ISO/CD 199.2. Blood-gas Exchangers(Oxygenators) 1993. Document ISO/TC 150/SC2/WG/N 103.